Figure S1

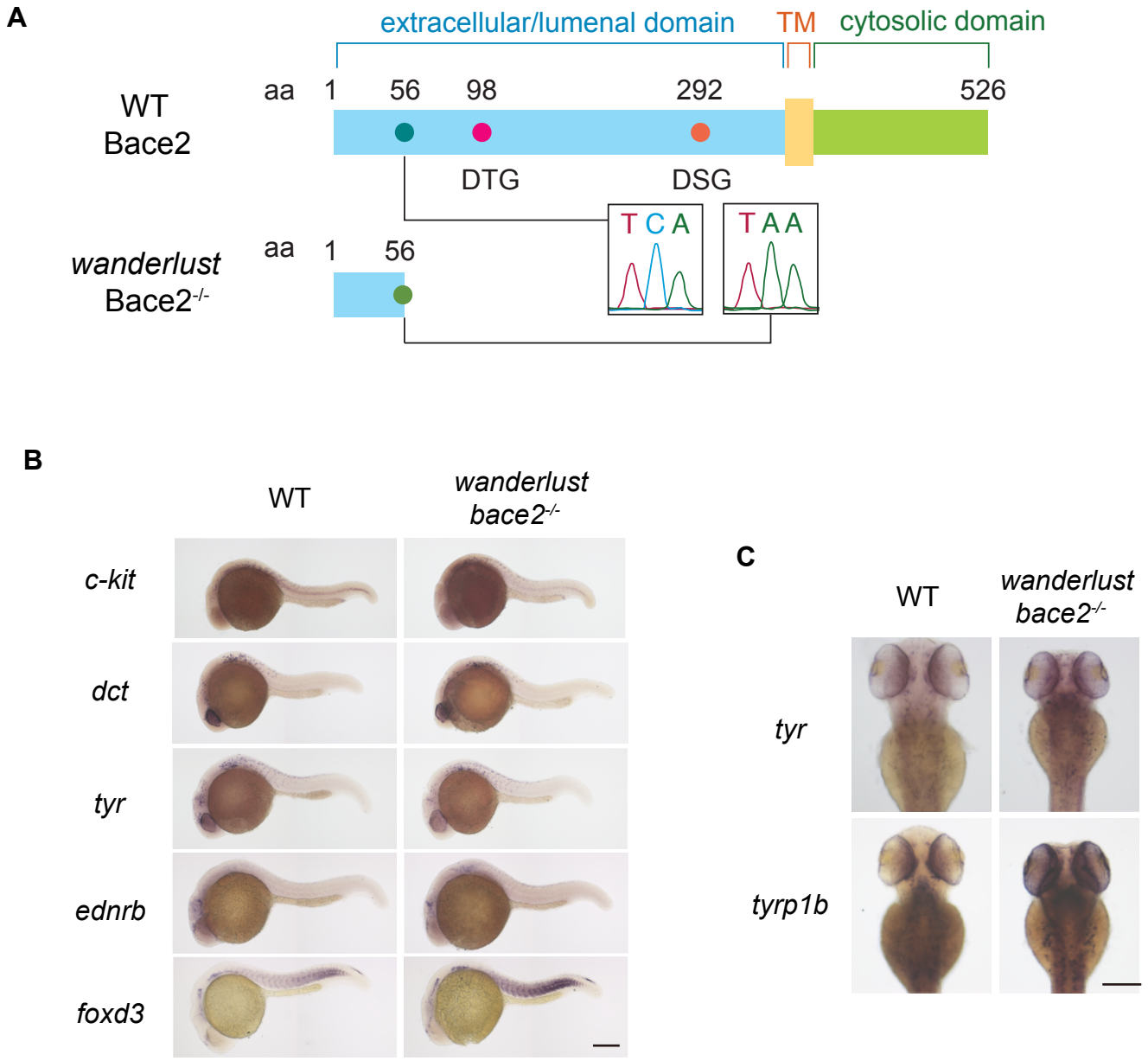

Figure S1. Related to Figure 1 and 2: *bace2*$^{-/-}$ mutants have increased mRNA expression of pigmentation genes.

(A) Schematic representation of zebrafish WT and Bace2$^{-/-}$ protein as found in the *wanderlust* mutant. Zebrafish Bace2 is a type I integral membrane β secretase that contains two DTG and DSG protease sites within its extracellular/lumenal domain. The *wanderlust* mutant (Bace2$^{-/-}$) has a C to A nonsense mutation leading to a truncated protein with size of 56 amino acids (aa), lacking both protease sites. TM=Transmembrane domain.

(B-C) ISH shows no detectable difference in neural crest or melanophore genes expression between WT and *bace2*$^{-/-}$ fish at 24 hpf (B), but ISH shows pigmentation genes are elevated in *bace2*$^{-/-}$ fish at 72 hpf (C). Scale bars, 200μM.

Figure S2

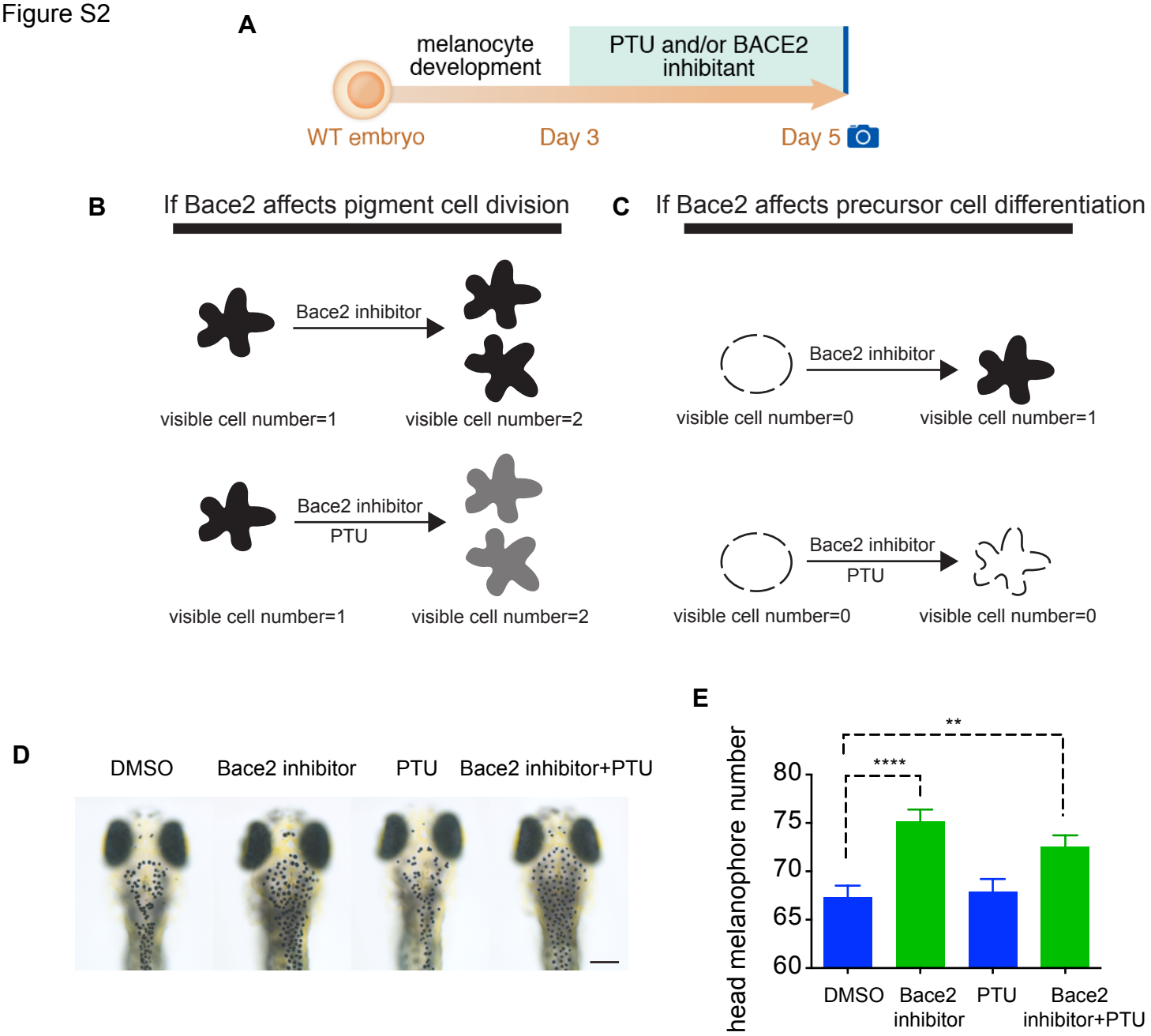

Figure S2. Related to Figure 2: Bace2 deficiency leads to increased melanophore cell division.
(A) Schema for testing the mechanism of increased melanophore cell number when Bace2 is loss. WT embryos were treated from 3-5dpF with 300μM PTU and/or 100μM Bace2 inhibitor (PF-06663195). PTU is a tyrosinase inhibitor that prevents new melanin synthesis to allow visualization only of previously pigmented melanophores.
(B-C) Schema for two possible scenarios. If Bace2 loss of function induces pigment cell division as shown in (B), co-treatment with the Bace2 inhibitor and PTU would still increase melanophore cell number the same way as Bace2 inhibitor treatment alone. This is because PTU would not affect pre-existing melanin and the newly derived daughter cells would inherit melanin from their mother cell. If Bace2 loss of function induces differentiation of unpigmented precursor cells as shown in (C), co-treatment with the Bace2 inhibitor and PTU would not increase visible melanophores cell number, as PTU would inhibit any new melanin from synthesis.
(D-E) Co-treatment with the Bace2 inhibitor and PTU led to an increase in the number of pigmented melanophores, which necessarily must have come from previously pigmented cells division due to the effects of PTU, quantified in (E). The data are from three independent experiments, one-way ANOVA followed by Holm-Sidak's multiple comparisons test; fish number n(DMSO)=53, n(Bace2 inhibitor)=56, n(PTU)=54, n(Bace2 inhibitor+PTU)=61. **P<0.01, ****P<0.0001. Epinephrine (5mg/ml) was used to aggregate melanin to facilitate cell counting. All bar graphs are presented as mean ± s.e.m. Scale bars, 200μM.

Figure S3

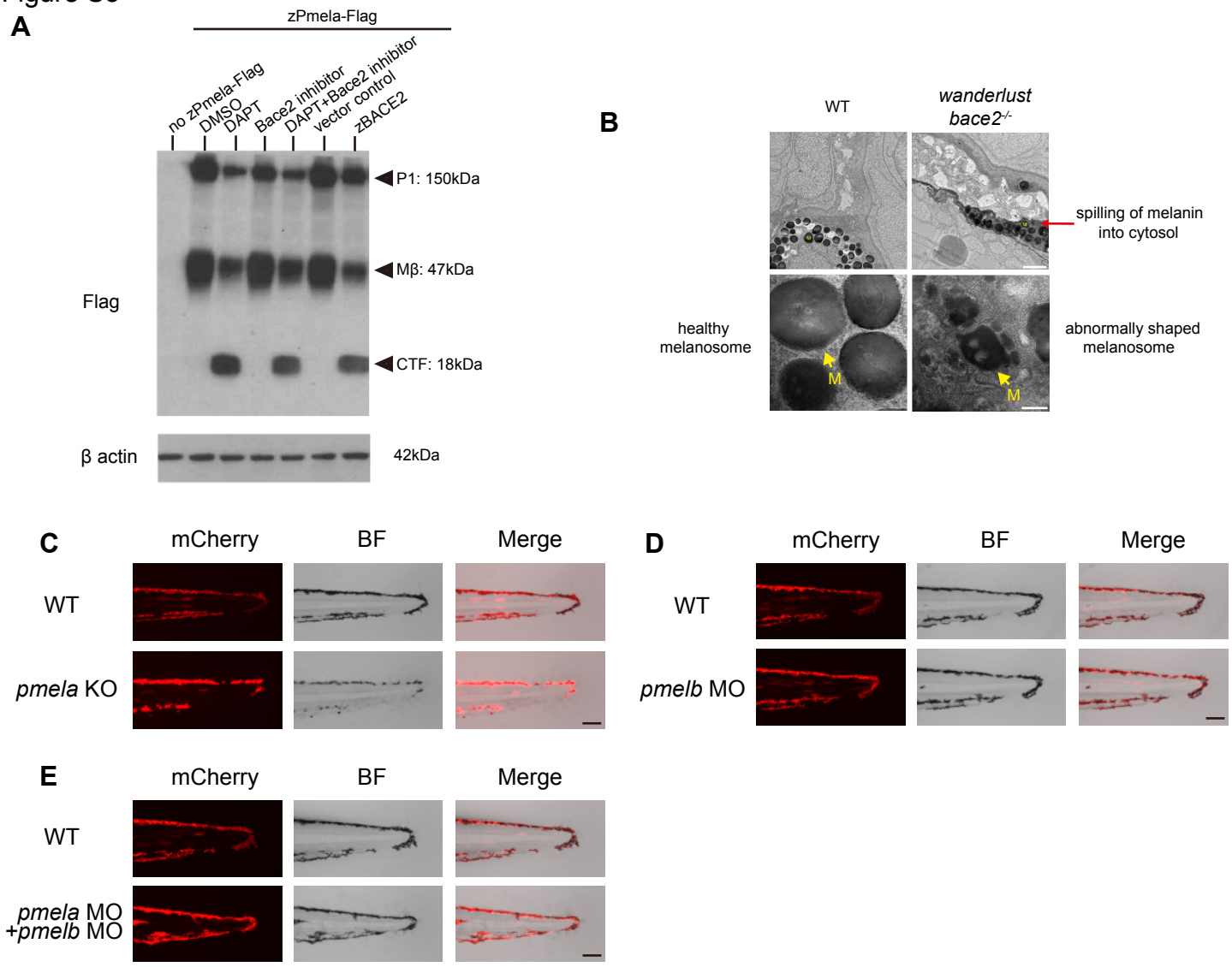

Figure S3. Related to Figure 4: Pmel is a substrate for Bace2 but is not responsible for the *wanderlust* phenotype.

(A) zebrafish Bace2 cleaves Pmela. We constructed a fusion protein of zebrafish Pmela and a C-terminal Flag tag to detect cleavage by immunoblotting using Flag antibody. Expression of the fusion protein in HEK 293T cells reveals an immature core-glycosylated P1 form of Pmela (~150 kDa), the Mβ (~47 kDa), and the CTF (~18 kDa) when treated with γ secretase inhibitor DAPT (1μM), in a similar manner to human PMEL protein. Inhibition of human BACE2 using BACE inhibitor IV (1μM) increases the relative abundance of Mβ and decreases the abundance of the CTF, suggesting Bace2 cleaves Mβ and gives rise to CTF. Co-expression of the fusion protein and zebrafish Bace2 (zBACE2) leads to accumulation of cleavage product CTF, suggesting zebrafish Bace2 is sufficient to cleave zebrafish Pmela.

(B) Electron microscopy of 72hpf embryos tail melanophores showed a difference in melanin distribution as well as melanosome (M) shape. Melanosomes in WT are round with a smooth outline and homogeneously filled with melanin (yellow arrow). *bace2*$^{-/-}$ melanophores have a darker hue in the cytosol (red arrow) and irregular melanosome membrane (yellow arrow), suggesting a leakage of melanin out of melanosomes into the cytosol.

(C) Knockout of *pmela* using CRISPR-Cas9 in WT zebrafish leads to pale but not dendritic melanophores, similar to previously published *fading vision* mutant. This suggests that loss of *pmela* does not result in hyperdendritic melanophores. Melanophore membrane structure is visualized using *Tg(tyrp1b: membrane-mCherry)* strain at 3dpF.

(D-E) Knockdown of *pmelb* alone (D) or co-knockdown of *pmela* and *pmelb* (E) using morpholinos in WT embryos does not lead to the hyperdendritic melanophore phenotype as seen in the *bace2*$^{-/-}$ mutant. Scale bars, 100 nM (B bottom panel), 1μM (B top panel), 100μM (C-E).

Figure S4

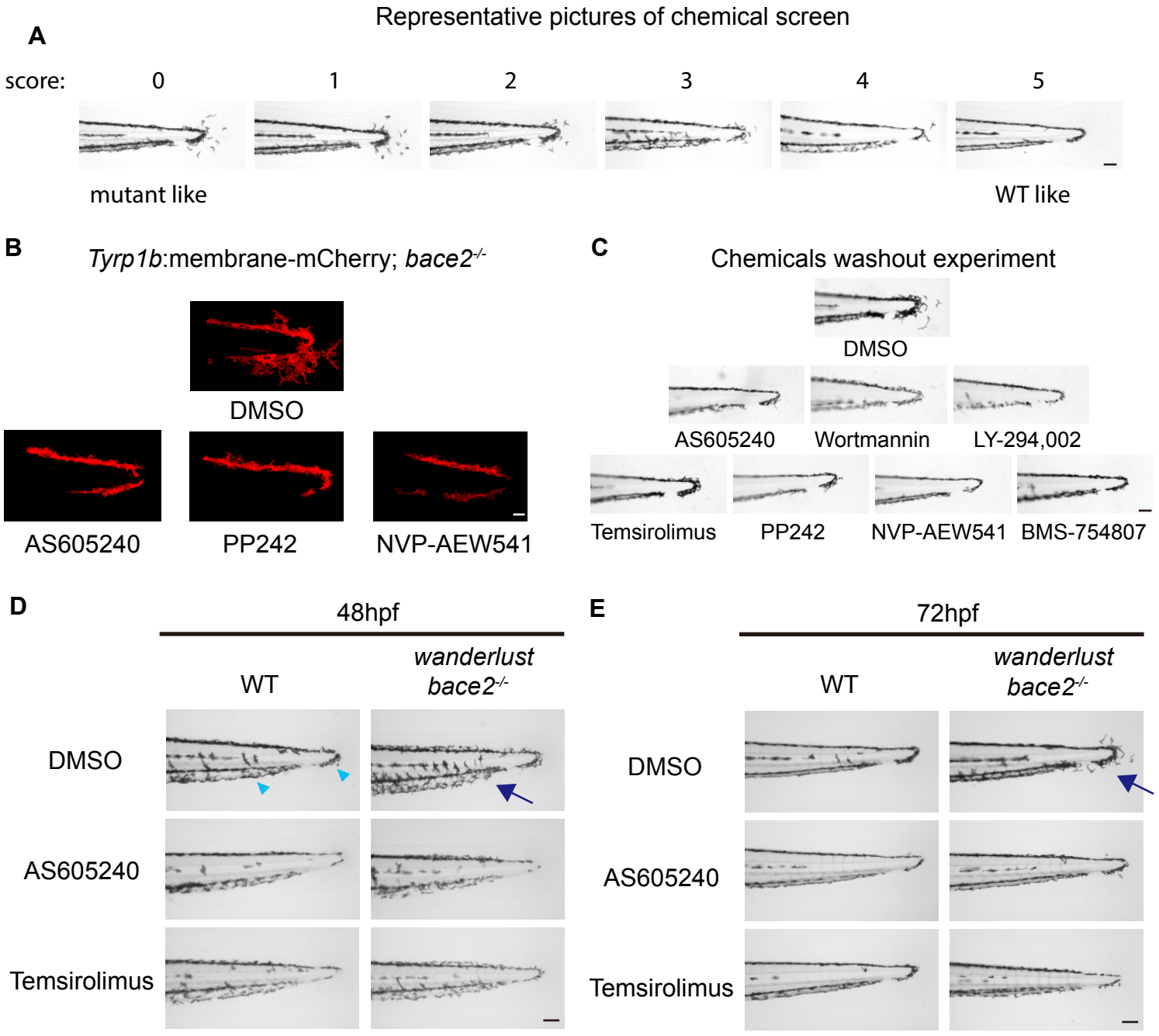

Figure S4. Related to Figure 4 and Figure 6: PI3K/mTOR inhibition rescues dendritic melanophores in *bace2*$^{-/-}$.

(A) Representative pictures of melanophores with chemical screen scores from 0 (non-rescued, mutant like) to 5 (fully rescued, WT like).

(B) Confocal pictures high magnification view of tailfin melanophores in response to PI3K inhibitor AS605240 (110nM), mTOR inhibitor PP242 (15μM) and insulin receptor inhibitor NVP-AEW541 (60μM). *Tg(tyrp1b: membrane-mCherry)* fish were treated from 24hpf to 72hpf to visualize melanophore membrane structure. Also see Supplemental Movie 1-4.

(C) PI3K/mTOR/Insulin receptor inhibitors effect on tail melanophore phenotype is not reversible by drug washout. *wanderlust* mutants were treated with inhibitors from 24hpf to 72hpf, then inhibitors were washed off extensively and embryos were imaged at 108hpf.

(D-E) *bace2*$^{-/-}$ is hypersensitive to PI3K/mTOR inhibition compared to WT fish. PI3K/mTOR inhibition reduced WT melanophore dendricity at 48hpf (D, arrowhead), but the *bace2*$^{-/-}$ melanophores are more sensitive to this effect at both 48hpf and 72hpf (D and E, arrow). Treatment of WT and *bace2*$^{-/-}$ embryos with the PI3K inhibitor AS605240 (110nM) or mTOR inhibitor Temsirolimus (30μM) from 24-48hpf (D) or from 24-72hpf (E). Scale bars, 30μM (B), 100μM (A, C, D, E).

Figure S5

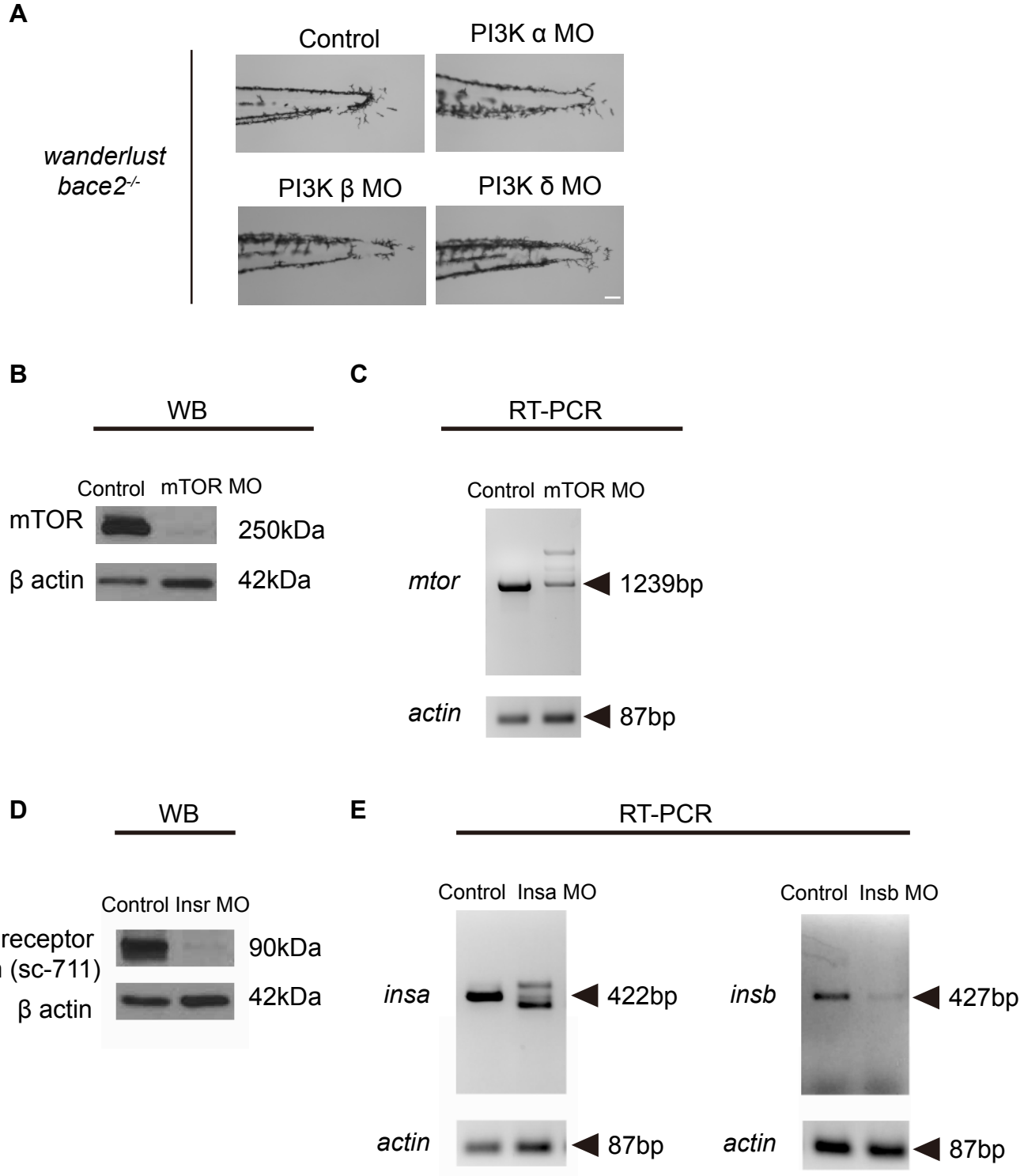

Figure S5. Related to Figure 4, 6, 7: Control experiments for morpholino knockdown.
(A) Knockdown of PI3K α, β or δ isoforms using morpholinos does not rescue *bace2*$^{-/-}$ dendritic melanophores to the same extent as PI3K γ morpholinos, as shown in Figure 4E.
(B) Knockdown of mTOR using mTOR splicing morpholino leads to depletion of mTOR protein in Western blot. Membrane probed with anti-mTOR antibody and β-actin as a loading control.
(C) RT-PCR shows knockdown of mTOR using mTOR splicing morpholino leads to abnormal mRNA splicing. *mtor* fragment is amplified using primers adjacent to morpholino target sites. *actin:* input control.
(D) Western blot shows co-knockdown of insra and insrb using morpholinos leads to decrease insulin receptor protein. Membrane probed with antibody sc-711 recognizing insulin receptor β chain and β-actin as a loading control.
(E) Knockdown of *insa* (Left) and *insb* (Right) using splicing morpholinos lead to abnormal mRNA splicing and expression in RT-PCR. Fragments are amplified using primers adjacent to morpholino target sites. *actin*: input control. Scale bars, 100μM.

Figure S6

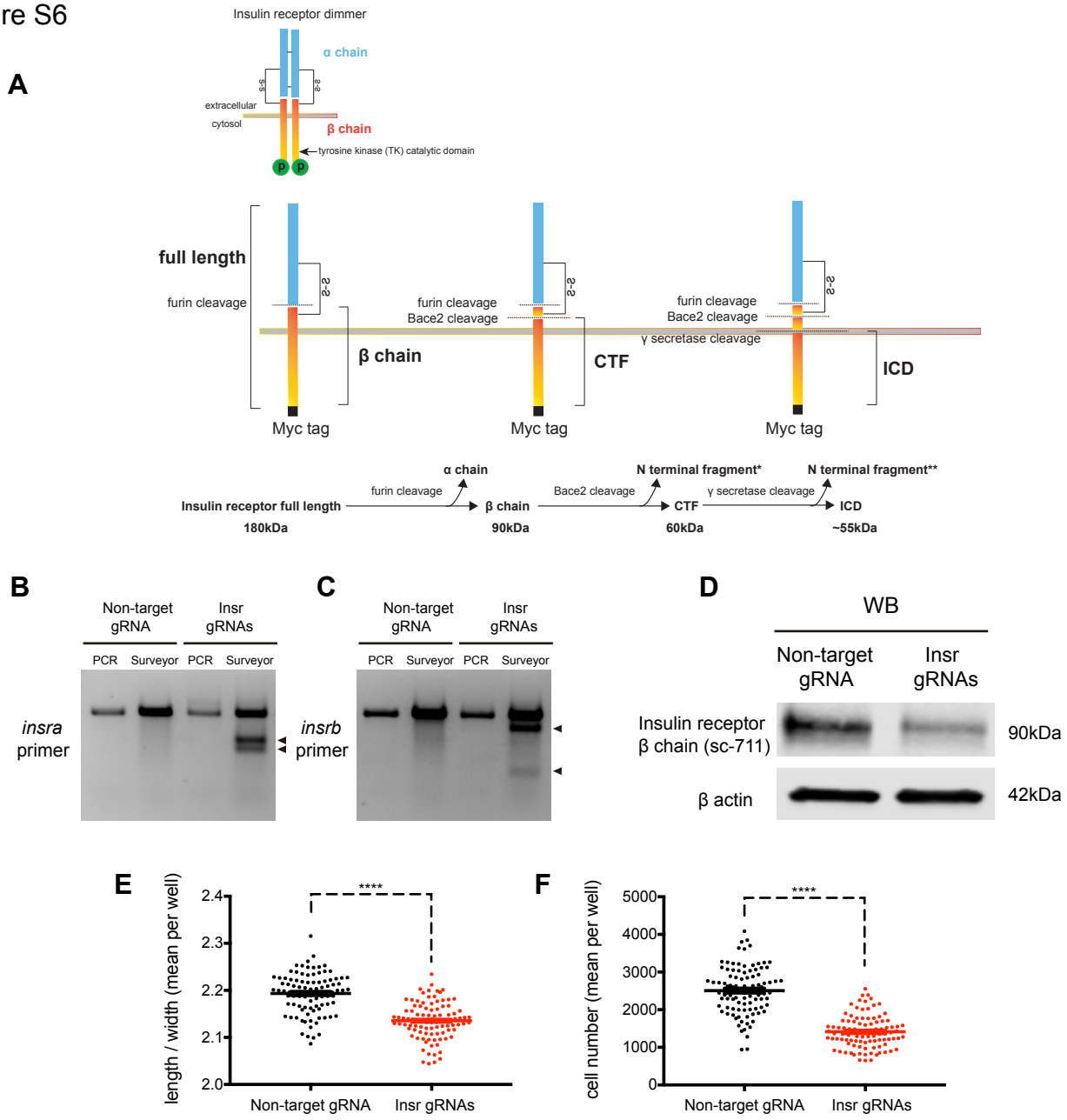

Figure S6. Related to Figure 6: Bace2 cleaves insulin receptor to regulate melanophore morphology and number.

(A) Schematic representation of the protease cleavage steps of the insulin receptor. Insulin receptors are dimerized to form a functional unit as shown in the top panel. The full length monomer is first cleaved by furin, to yield the α and β chains. The β chain is then cleaved by Bace2 to yield the C-terminal fragment (CTF), which is then cleaved by γ secretase. When Bace2 is abundant, there is an accumulation of the CTF as cleavage product (as shown in Figure 6E-F). When Bace2 is inhibited, there is an accumulation of the β chain (as shown in Figure 6G-H). The ICD is not detectable in this experiment because it is unstable and quickly degraded by proteasome. (B-F) Insulin receptor regulates melanophore morphology and number in ZMEL1 cells. Two guide RNAs (gRNAs) targeting zebrafish *insra* and *insrb* respectively were co-nucleofected into ZMEL1 cells together with tracrRNA and recombinant Cas9 nuclease. A non-targeting gRNA was included as negative control. Surveyor nuclease assay was used to detect mutations in the *insra* (B) and *insrb* (C) genomic locus, resulting in two smaller digested PCR bands at the expected sizes (arrowhead). (D) Western Blot shows a pooled ZMEL1 knockout population leads to reduced Insr protein level. Membrane probed with antibody sc-711 recognizing insulin receptor β chain and β-actin as a loading control. Knockout of both insulin receptors in ZMEL1 cell using Crispr-Cas9 leads to less elongated/dendritic cell morphology (E) and reduced cell number (F), data are from three independent experiments. All bar graphs are presented as mean ± s.e.m. two-tailed t test, ****P<0.0001.

Figure S7

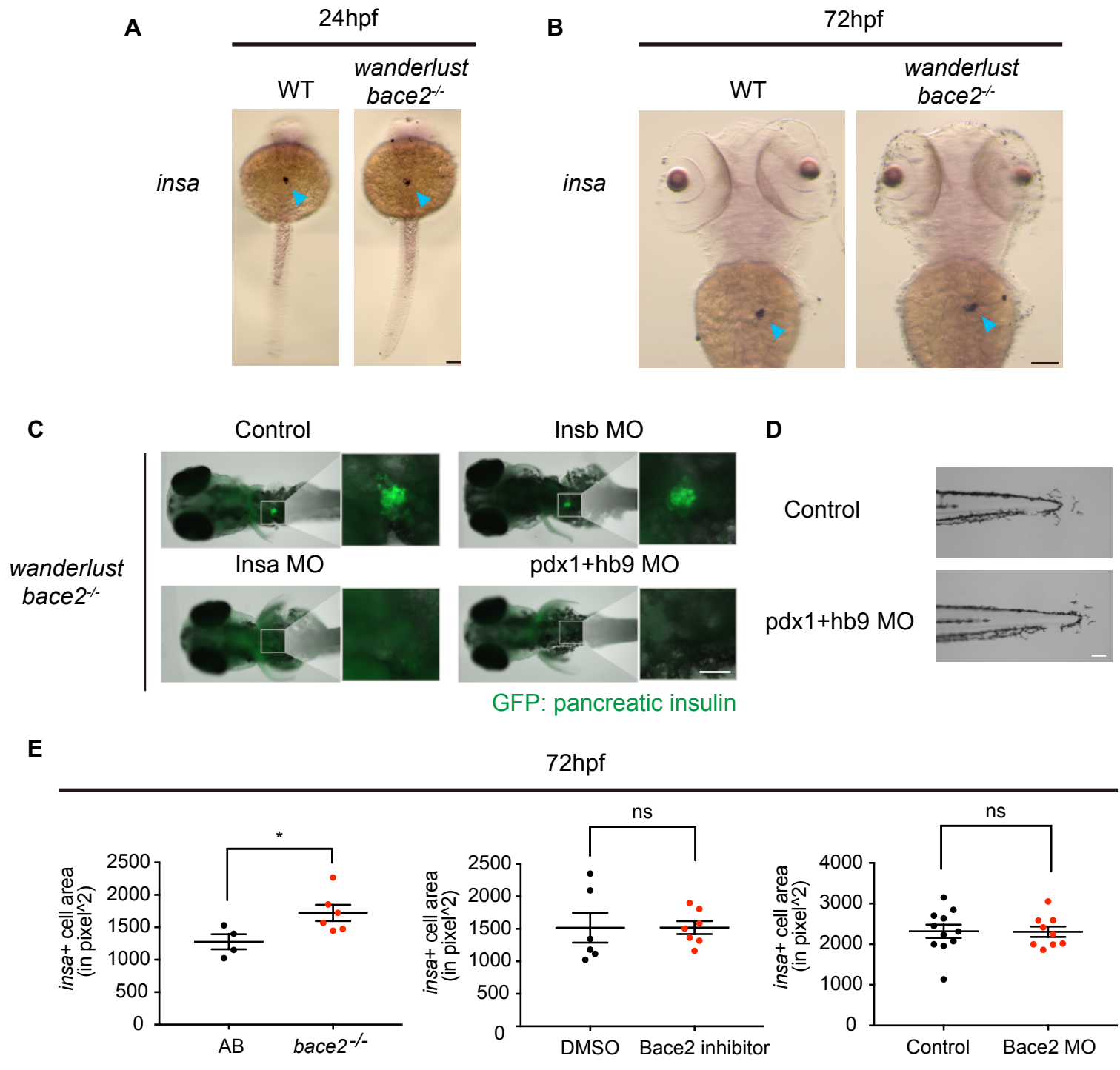

Figure S7. Related to Figure 7: Pancreatic *insa* ablation does not rescue the *bace2*$^{-/-}$ phenotype.

(A-B) ISH shows *insa* mRNA is specifically expressed in pancreas at 24hpf (A) and at 72hpf (B) for both WT and *bace2*$^{-/-}$ embryos (arrowhead).

(C) Immunostaining shows knockdown of either *insa* or *pdx1/hb9* in *bace2*$^{-/-}$ mutants completely ablates insulin staining in the pancreas, while *insb* knockdown does not change pancreatic insulin level at 72hpf. Whole embryos were stained with anti-insulin antibody.

(D) Co-knockdown of *pdx1* and *hb9* in *bace2*$^{-/-}$ mutants fails to rescue dendritic melanophores at 72hpf.

(E) *wanderlust* mutant have slightly increased *insa* positive cell area compared to WT embryos at 72hpf, but Bace2 inhibitor and Bace2 morphant do not show significant differences to the control group, suggesting Bace2 loss of function does not consistently alter pancreatic β cell mass at 72hpf. n=each fish, two-tailed t test, *P<0.05. All bar graphs are presented as mean ± s.e.m. Scale bars, 50μM (C), 100μM (A, B, D).

MO Name	Working conc.	MO Sequence (5'-3')	Reference
Bace2 splicing MO	0.16mM	GTTACCACATAACATACCGTTTGTC	This paper
PI3K γ ATG MO	1mM	CATCATCACTGGCTTGCTGTTCCAT	Li et al., 2015
mTOR splicing MO	1mM	GGTTTGACACATTACCCTGAGCATG	Makky et al., 2007
Insra ATG MO	0.5mM	CAAAGTCCGCAGCCGCATTTTGACC	Wan et al., 2014
Insrb ATG MO	0.1mM	TGTGTCCAGCCGCATTCTGCCTCGC	Wan et al., 2014
Insa splicing MO	0.5mM	CCTCTACTTGACTTTCTTACCCAGA	Ye et al., 2016
Insb splicing MO	0.25mM	AAGTTGGAGACGTTGCTCACCCAGC	Ye et al., 2016
Pdx1 ATG MO	0.45mM	GATAGTAATGCTCTTCCCGATTCAT	Kimmel et al., 2011
Hb9 ATG MO	0.45mM	TTTTTAGATTTCTCCATCTGGCCCA	Kimmel et al., 2011
PI3K α ATG MO	1mM	GTCTTGGAGGCATGATTTGTAATCC	Li et al., 2015
PI3K β ATG MO	1mM	GCATGGCAGAGAACACACTGAAGCC	Li et al., 2015
PI3K δ ATG MO	1mM	GGCATCGTGCAGGAAAACTCATCTAC	Li et al., 2015
Pmela ATG MO	0.1mM	GAGGAAGATGAGAGATGTCCACATG	Schonthaler et al., 2005
Pmelb ATG MO	0.2mM	GTAGAGAATAGCTTCATTGTGTCAC	Burgoyne et al., 2015

Table S1. Related to STAR Methods: morpholinos working concentration, sequence and reference information.

Primer	Sequence (5'-3')
bace2 genotype F1	TCCTTGTTGCAGTCTATCCCT
bace2 genotype R1	GCACTTGAACTCCTCAGTTACA
mTOR MO F1	GAGTTCATGTTCCTGCTG
mTOR MO R1	CCATCCAATGTAGCATTGG
Insa MO F1	CATTCCTCGCCTCTGCTTC
Insa MO R1	GGAGAGCATTAAGGCCTGTG
Insb MO F1	CAGACTCTGCTCACTCAGGAAA
Insb MO R1	GCGTGTAATGGTCATTTATTGC
Tyrp1b ISH F1	TGGATAACCGTATTACCGCC
Tyrp1b ISH R1	CGCGCAATTAACCCTCACTAAAGCACTAGTCATACCAGGATC
Bace2 ISH F2	CACCATGCGGCTCTACGGGCTACTG
Bace2 ISH R2	CGCGCAATTAACCCTCACTAAAGAGTCACTCACTTGATGCGATGGCGCA
Insa ISH F1	TGTACGGAAGTGTTACTTCTGCTC
Insa ISH R1	GGATCCATTAACCCTCACTAAAGGGAAGGCCGCGACCTGCAGCTC
Insb TOPO F3	AGGTGTGGCTGTTGGTGAAT
Insb TOPO R3	CTGGCTGTTCAGCTGCAGTA
Insb ISH F1	AGGTGTGGCTGTTGGTGAAT
Insb ISH R1	GGATCCATTAACCCTCACTAAAGGGGAATTCGCCCTTCTGGCTG
Insra CRISPR F1	ATGTGACTCTGTGTTCTGTGCC
Insra CRISPR R1	TGCAGAATGCTGATTAACCAAT
Insrb CRISPR F1	GCCTATGCTCTCGTCTCACTCT
Insrb CRISPR R1	CCCATGTGTTTCATTCTAGCTG
bace2 pENTR/D-TOPO F1	CACCATGCGGCTCTACGGGCTACTG
bace2 pENTR/D-TOPO R1	CTTGATGCGATGGCGCACCAAAGA
insra pENTR/D-TOPO F1	CACCATGCGGCTGCGGACTTTGATT
insra-pENTR/D-TOPO-R1	AGAAGGGGTGGATCGGGGTAGAG
insrb pENTR/D-TOPO F1	CACCATGCGGCTGGACACATCTGTGG
insr pENTR/D-TOPO R1	GGACGGACTAGATCTGGGTAAAGACAG
pmela cDNA F1	CGATTTAAAGCTATGCACCATGTGGACATCTCTCATCTTCCT
pmela cDNA R1	ATCATCCTTGTAATCCACCACGCGTCCCAGCAGAAGT

Table S2. Related to STAR Methods: primer sequence.

ISH probe	Source	Reference
Dct	Gift from David Parichy (University of Virginia)	Kelsh et al., 2000
Mitfa	Gift from David Parichy (University of Virginia)	Lister et al., 1999
Tyr	Gift from David Parichy (University of Virginia)	Mellgren and Johnson, 2004
Sox10	Gift from David Parichy (University of Virginia)	Dutton et al., 2001
Crestin	Gift from David Parichy (University of Virginia)	Luo et al., 2001
c-kit	Gift from David Parichy (University of Virginia)	Parichy et al., 1999
Pmela	Gift from James Lister (Virginia Commonwealth University)	Schonthaler et al., 2005
ednrb1a	Gift from James Lister (Virginia Commonwealth University)	Parichy et al., 2000
Tyrp1b	Thermo Fisher Scientific	cat # EDR1052-210947471
Bace2	This paper	
Foxd3	Gift from James Lister (Virginia Commonwealth University)	Odenthal and Nüsslein-Volhard 1998
Insa	Dharmacon	cat # MDR1734-202792960
Insb	This paper	Reference sequence: Junker et al., 2014

Table S3. Related to STAR Methods: *in situ* hybridization (ISH) probes, source and reference.